CHAPTER 5

5.1 Introduction

One of the main frontier of the current science is the miniaturisation of devices through the dimensional reduction of their singular components. The recent developments of supramolecular chemistry[1] have indeed extended the concept of machines and devices down to the molecular level.[2] A *molecular machine* is defined as *an assembly of a number of molecular components that makes mechanical movements, designed to perform machine-like motions in response to appropriate external stimuli (chemical, photonics electrochemical etc.).*[2] In this wide field several molecular components have been successfully used to devise molecular machines. Among them, those belonging to the classes of *rotaxanes* and *pseudorotaxanes* seem to offer a wider potentiality.[2,3]

In simple instances, a rotaxane is a mechanically-interlocked molecular architecture consisting of a dumbbell-shaped district that is threaded through a macrocycle or a ring-like component (see figure 5.1). The two components are kinetically trapped as the two end-groups of the dumbbell (the stoppers) are larger than the internal diameter of the ring, thus preventing the dissociation (dethreading) of the components since this would require significant distortion or cleavage of covalent bonds.

---

1. a) J.-M. Lehn, *Angew. Chem. Int. Ed. Engl.* **1988**, *27*, 89; b) J.-M. Lehn, *Supramolecular Chemistry: Concepts and Perspectives*, VCH, Weinheim, **1995**.
2. V. Balzani, A. Credi, M. Venturi, *Molecular devices and machines- A journey into the nano world* ,Wiley-VCH, Germany, **2003**.
3. V. Balzani, A. Credi, F. M. Raymo, J. F. Stoddart, *Angew. Chem. Int. Ed.* **2000**, *39*, 3348.

When the thread bears only one or no stopper, the system is a supramolecular complex the thermodynamic stability of which is dictated by the magnitude and nature of the non covalent intermolecular interactions that take place upon complex formation. This latter type of supramolecular complex is termed a pseudorotaxane.[4]

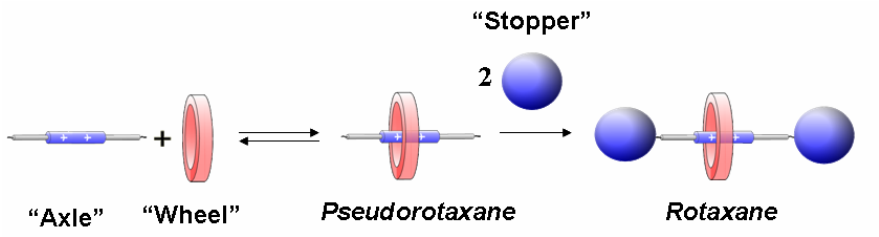

Figure 5.1. Schematic representation of pseudorotaxane and rotaxane

In this field one of the promising goal is to create molecular machines that can work or move in a particular desired way by a particular external stimuli such as pH variation, oxidation/reduction or by photoinduction. In the following example (see Figure 5.2)[5] a [2]-rotaxanes moves along his dumbbell-shaped component. Its movement is controlled by the electrochemically oxidation/reduction of the Cu metal centre.

4. See *e. g.*: a) P. R. Ashton, I. Baxter, M. C. T. Fyles, F. M. Raymo, J. F. Stoddart, A. J. P. White, D. J. Williams, *J. Am. Chem. Soc.* **1988**, *120*, 2297; b) M. Asakawa, P. R. Ashton. R. Ballardini, V. Balzani, M. Belohradsky, M. T. Gandolfi, O. Kocian, L. Prodi, F. M. Raymo, J. F. Stoddart, M. Venturi, *J. Am. Chem. Soc.* **1997**, *119*, 302; c) F. M. Raymo, J. F. Stoddart, *Chem. Rev.* **1999**, *99*, 1643; d) *Molecular Catenanes, Rotaxanes and Knots*, Eds.: J.-P. Sauvage, C. O. Dietrich-Buchecker, Wiley-VCH, Weinheim, **1999**.

5. N. Armaroli, V. Balzani, J.-P. Collins, P. Gaviña, J.-P. Sauvage, B. Ventura, *J. Am. Chem. Soc.*, **1999**, *121*, 4397

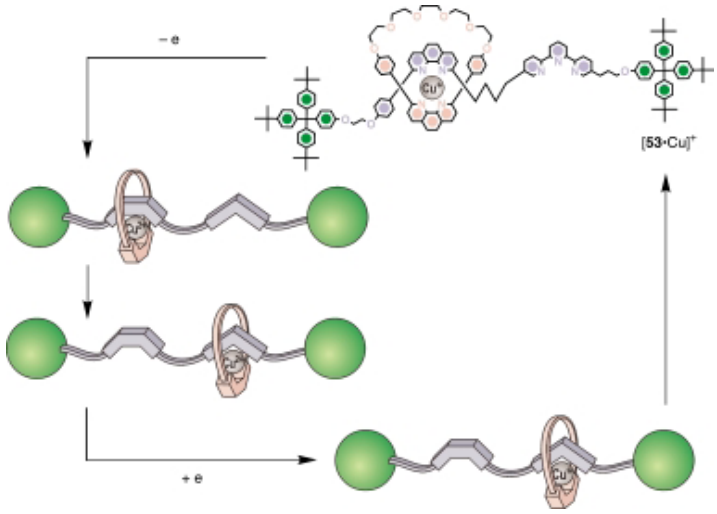

Figure 5.2. An example of a movement of dumbbell component in a [2]-rotaxane mediate by electrochemical stimuli

The possibility to transfer the theoretical achievements gained in this field to practical applications is obviously challenging. To this aim, an approach that is under extensive evolution is the anchoring of rotaxanes and pseudorotaxanes to solid surfaces.[6] Less attention has been devoted to the synthesis of rotaxanes and pseudorotaxanes anchored to metal surfaces in MPCs. These systems have as big advantage with respect surfaces that they can be conveniently studied both in solution and with microscopy techniques. Some examples of polipseudorotaxanes and rotaxanes on gold MPCs are present in the literature,[7] however, the species used as components in these structures have been always not electrochemical active.

In the recent years our research group has extensively used a triphenyluriedo calix[6]arene derivative as a wheel for the synthesis of

6. See *e.g.* : a) T. J. Hubin, D. H. Busch, *Coord. Chem. Rev.*, **2000**, 5; b) J. F. Stoddart, *Acc. Chem. Res*., **2001**, 34 and references therein.
7. Y.-L. Zhao, Y. Cheng, M. Wang, Y. Liu, *Org. Lett.* **2006**, *8*, 1267

rotaxanes and pseudorotaxanes[8] (see Figure 5.3) with axles based on derivatives of 4,4'-bipyridinium salt (viologens). These compounds are known as a electrochemical active specie.[9]

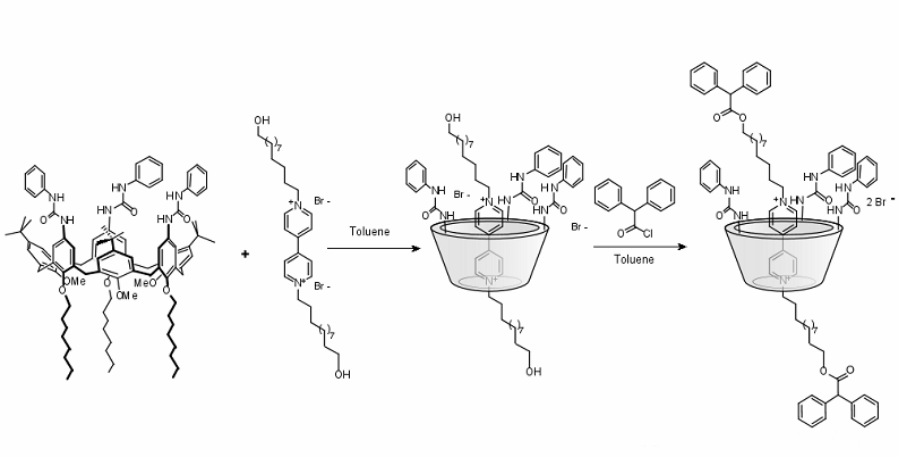

Figure 5.3. Formation of a calix[6]arene-based rotaxanes

Calix[6]arene derivatives such as that depicted in figure 5.3 have as important peculiarity a truncated cone structure where an axle could, in principle, enter form the narrower or wider side, giving rise to oriented pseudorotaxanes or rotaxanes characterized by the univocal orientation of the wheel side with respect to the two termini of the axial component. Our research group has shown that it is possible to govern the threading process from the macrocycle upper rim using monostoppered

8. a) A. Arduini, R. Ferdani, A. Pochini, A. Secchi, F. Ugozzoli, *Angew. Chem. Int. Ed.* **2000**, *39*, 3453; b) A. Arduini, F. Calzavacca, A. Pochini, A. Secchi, *Chem. Eur. J.* **2003**, *9*, 793; c) F. Ugozzoli, C. Massera, A. Arduini, A. Pochini, A. Secchi, *Cryst. Eng. Comm.*, **2004**, 6, 227; d) A. Credi, S. Dumas, S. Silvi, M. Venturi, A. Arduini, A. Pochini, A. Secchi, *J. Org. Chem.* **2004**, *69*, 5881.

9. See *e.g.*: P. S. M. Monk, *The Viologens: physicochemical properties, synthesis and applications of the salts of 4,4'-bipyridine*, John Wiley & Sons, Chichester, **1998**.

asymmetrical axle to yield oriented pseudorotaxanes[8b] and rotaxanes.[10] This behaviour was explained on the basis of the following observations: i) in low polar media the bipyridinium-based axles are present as tight ion pairs that cannot enter into the calix[6]arene cavity; ii) in low polar media the access of the axle into the cavity from the lower rim is prevented for sterical reasons by the inward orientation of the three methoxy groups present on the rim; iii) the access of the axle from the upper rim is favoured by the presence of three hydrogen bond donor ureido groups that are able to separate the ion-pair, thus pivoting the entrance of the bipyridinium axle into the cavity (see Figure 5.4).[8b,10]

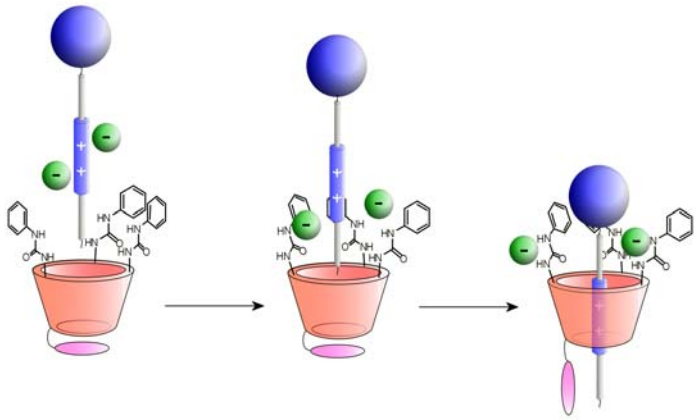

Figure 5.4. Schematic representation of the selective threading process of viologen-based axle through the upper rim of tri-phenylureido-calix[6]arene-based wheel (the violet oval represents the three methoxy groups present onto the macrocycle lower rim).

The access to the cavity can be also controlled varying the polarity of the media where the threading process is carried out. In more polar media like acetonitrile, the threading process occurs also from the lower rim and it is thus possible to obtained almost equimolar mixture of the two

10. A. Arduini, F. Ciesa, M. Fragassi, A. Pochini, A. Secchi, *Angew. Chem. Int. Ed.* **2005**, *44*, 278.

different oriented pseudorotaxanes that can than be converted after the stopping reaction in the respectively mixture of the two oriented rotaxanes (see Figure 5.5).

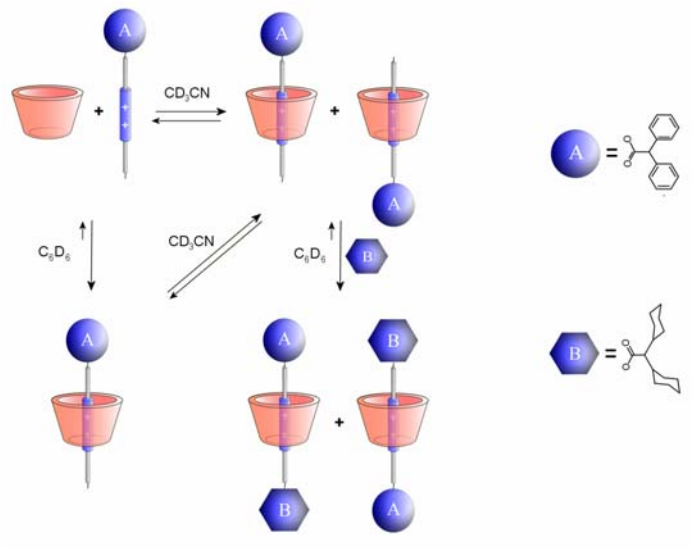

Figure 5.5 Synthesis of both constitutionally isomeric oriented calix[6]arene-based rotaxanes in acetonitrile

5.2 Rotaxanes and pseudorotaxanes supported on semiconductor (CdSe) nanoparticles and Au clusters

The interesting results obtained in the preparation of Au MPCs stabilized with calix[4]arene derivatives (see Chapters 3 and 4), prompted us to explore the possibility to combine the properties of pseudorotaxane and rotaxane structures derived from calix[6]arenes with those derived by metallic clusters and semiconductor nanoparticles (quantum dots).

5.2.1 Synthesis of thiolated calix[6]arene "wheel"

The insertion of a calix[6]arene "wheel" as monolayer for a metallic surface either of semiconductor nanoparticles based on CdSe or Au clusters requires as usual the presence in the macrocycle platform of some thiol functional groups that can act as anchoring points. To this aim the calix[6]arene "wheel" **8** (see Formula) was designed. It is characterized by three phenylureido groups at its upper rim and by the presence of three long thiolated alkyl chains at its lower rim.

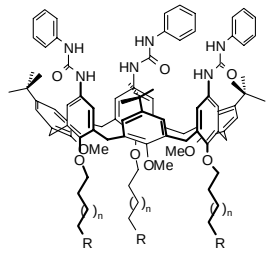

8 n=8, R=SH

As seen in chapter 3, the introduction of thiol groups in simple calix[n]arene derivatives is usually performed functionalizing the macrocycle lower rim with long ω-alkenyl chains, followed by insertion of the thiol group via radical addition of thioacetic acid. On the other hand, the introduction of the phenylureido groups in the calix[6]arene skeleton is usually accomplished starting from tri-nitro derivatives through their reduction to the corresponding tri-amino compounds followed by reaction with phenylisocyanate.[8] Although several attempts were made, this reduction step was not chemically compatible with the insaturations present in the alkyl chains. Therefore, the thiolated calix[6]arene **8** has been prepared from the known trinitro-calix[6]arene

precursor **1**,[11] following a synthetic pathway (see scheme 5.1), which involves several protection and deprotection steps of the thiol groups.

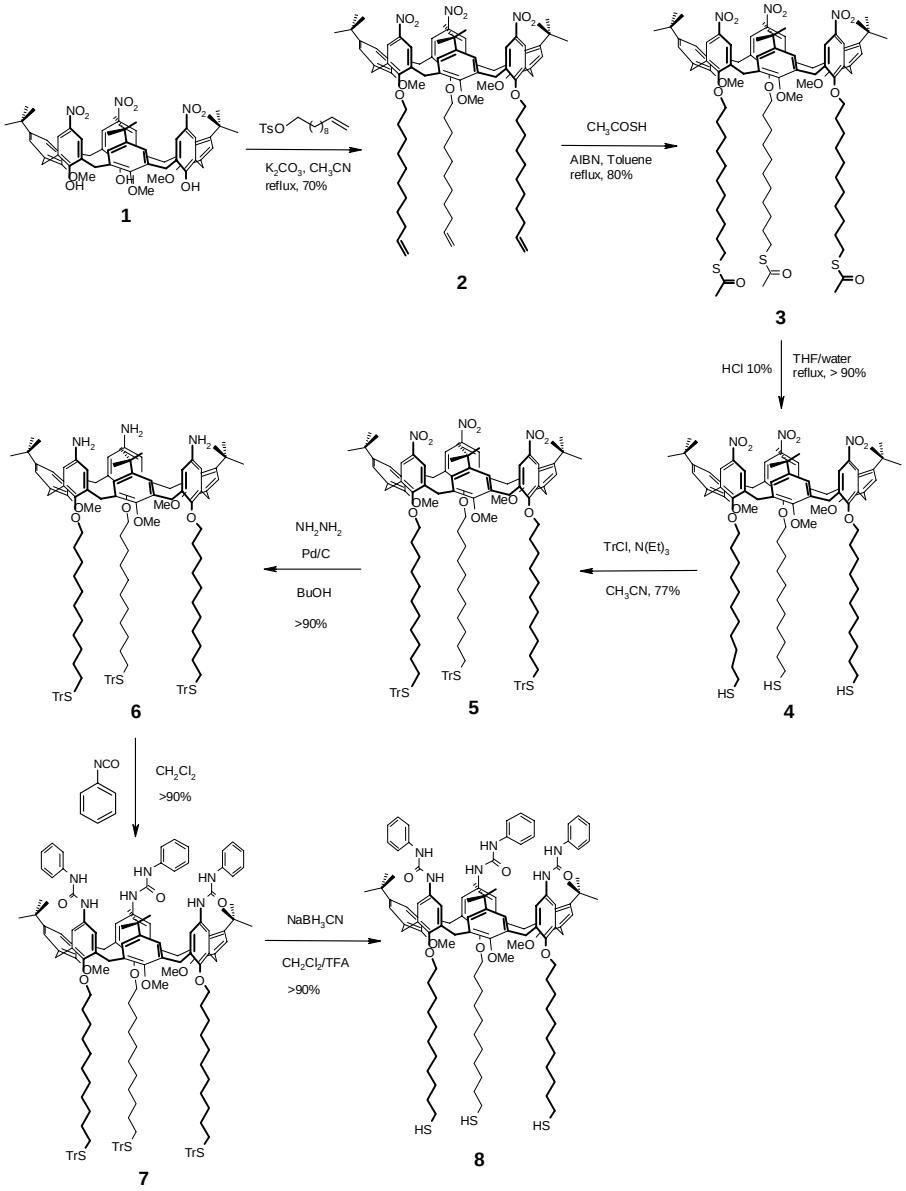

Scheme 5.1

11. J. J. Gonzales, R. Ferdani, E. Alberini, J. M. Blasco, A. Arduini, A. Pochini, P. Prados, J. De Mendoza, *Chem. Eur. J.* **2000**, *6*, 73

In particular, **1** has been alkylated at its lower rim with toluene-4-sulfonic acid undec-10-enyl ester using K_2CO_3 as base in refluxing acetonitrile. The thiols were then introduced as thioacetyl ($SOCH_3$) groups on the terminal insaturation of the alkyl chains of **2** through a radical anti-Markovnikov addition of thioacetic acid, mediated by the radical initiator AIBN. After acid hydrolysis (HCl) of the thioacetyl groups of **3**, the resulting free thiol groups of **4** have been alkylated in acetonitrile with trityl chloride, using triethylamine as proton scavenger. The nitro groups of **5** have been then reduced with hydrazine, in the presence of catalytic amounts Pd(0). The resulting amino groups of **6** were then reacted with phenylisocyanate in CH_2Cl_2 to afford **7** in quantitative yield. Finally, removal of the trityl protecting groups of **7** with $NaBH_3CN$ and trifluoro acetic acid afforded the target molecule **8** in almost quantitatively yield. The trityl group has been chosen as protecting group of the sulphur termini because it is stable in basic condition (reduction step $NO_2 \rightarrow NH_2$ mediated by hydrazine). Trityl sulphur deprotection is usually carried out using a silane compound ($HSiEt_3$) as hydride donor.[12] However, these reaction conditions determined a partial cleavage of the methoxy groups present on the calix[6]arene lower rim of **7**. Better deprotection compatibility was instead found using sodium cyanoborohydride as source of hydride ions.

The NMR spectrum of **8** (see Figure 5.6) present several diagnostic signals for a calix[6]arene compound assuming on the NMR timescale a so-called *pseudo cone* conformation. Indeed, the "axial" and "equatorial"

12. D. A. Person, M. Blanchette, M. L. Backer, C. A. Guidon, *Tetrahedron Lett.* **1989**, *30*, 2739.

protons of the "bridging" methylene groups give rise to two broad doublet at δ = 4.37 and 3.55 ppm, respectively. The three OCH_3 resonate as very broad signal at δ = 2.8 ppm. This resonance is upfield shifted respect the usual value for this type of protons (≈ 3.8 ppm) since the methoxy are oriented, on the NMR timescale, inward the calix[6]arene cavity, thus experiencing a shielding anisotropic effect of the aromatic rings.

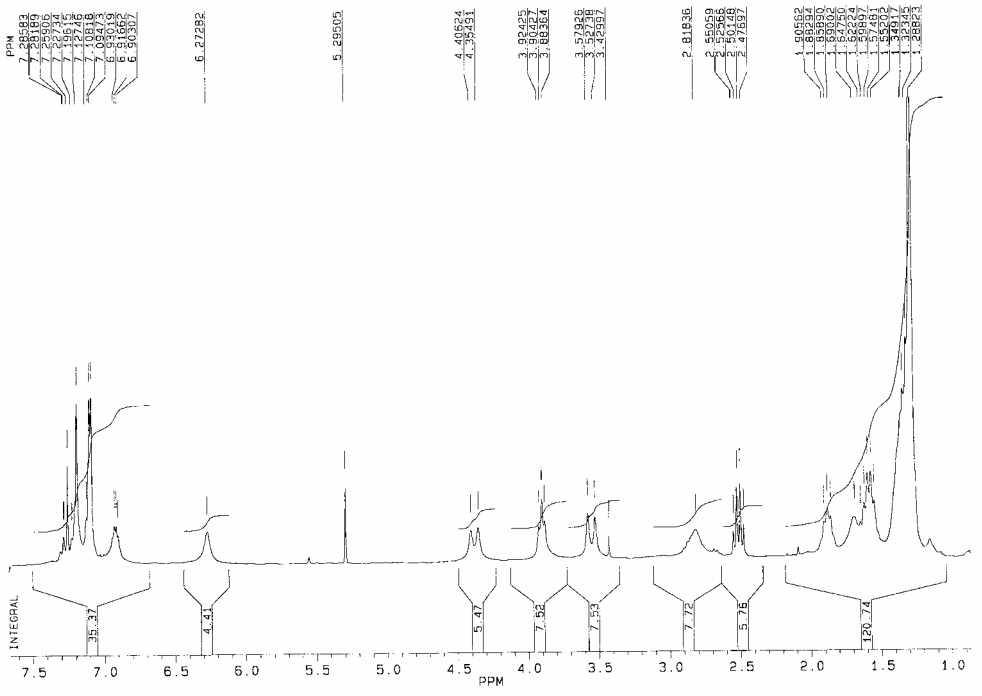

Figure 5.6. ^1H NMR (300 MHz) of calix[6]arene **8** in $CDCl_3$

The functionalization of the lower rim with the thiolated alkyl chains was confirmed by the presence in the upfield region of the spectrum of several characteristic multiplets (from 2.0 up to 1.4 ppm) corresponding to the methylene groups of the three alkyl chains. The multiplet centred δ = 2.51 ppm and integrating for six protons corresponds to the three methylene groups in α to each SH group. Its multiplicity and chemical

shift is diagnostic for the presence of deprotected SH groups (see chapter 3). The three ^{t}Bu groups of the upper rim resonate as singlet at δ = 1.29 ppm. The substitution of remnants aromatic nuclei with the phenylureido units was confirmed by the presence in the downfield region of the spectrum of the NH broad signals (6.27 ppm).

Although each step of the "sequential" synthetic approach used for the synthesis of **8** (see scheme 5.1) was characterized by good yields, the full pathway was really time demanding and afforded **8** in only ≈ 25% of overall yield. Therefore, a new "convergent" synthetic method has been developed (see Scheme 5.2). It was based on the synthesis of a new alkylating agent (**9**) in which the thiol group was already protected with the trityl PG. In particular, 11-bromoundecan-1-ol was alkylated with triphenylmethanethiol to give 11-(tritylthio)undecan-1-ol. This compound was used as such and converted in the *p*-tolyl 11-(tritylthio)undecyl sulfate **9** in 90% overall yield.

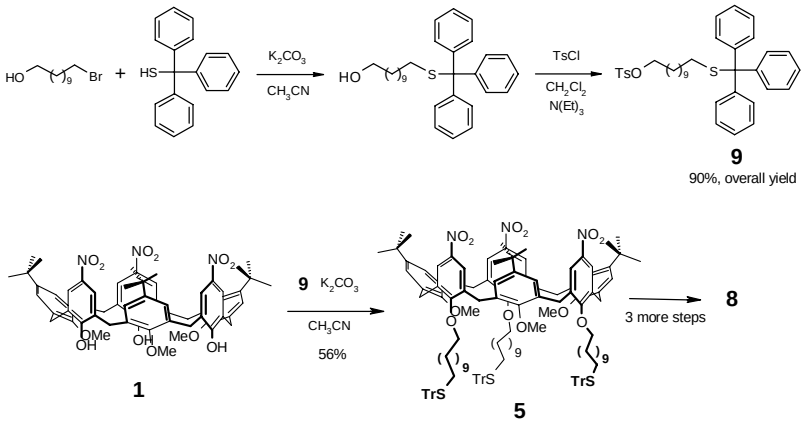

Scheme 5.2.

The ^{1}H NMR spectrum of **9** (see Figure 5.7) shows all the characteristic signals of the undecanyl chain, that is: three multiplets from 1.7 to 1.2 ppm corresponding to the inner methylene groups of the chain, a triplet at δ = 4.02 ppm for the CH_2 protons in α to the oxygen atom of the tosyl group, and a triplet at δ = 2.14 ppm for the CH_2 protons in α to the trityl protected sulphur atom. The trityl group gives rise to several crowded resonances in the aromatic region; moreover are present the diagnostic signals relative to the tosyl group at 2.44 (s), 7.79 (d) and 7.22 (d) ppm.

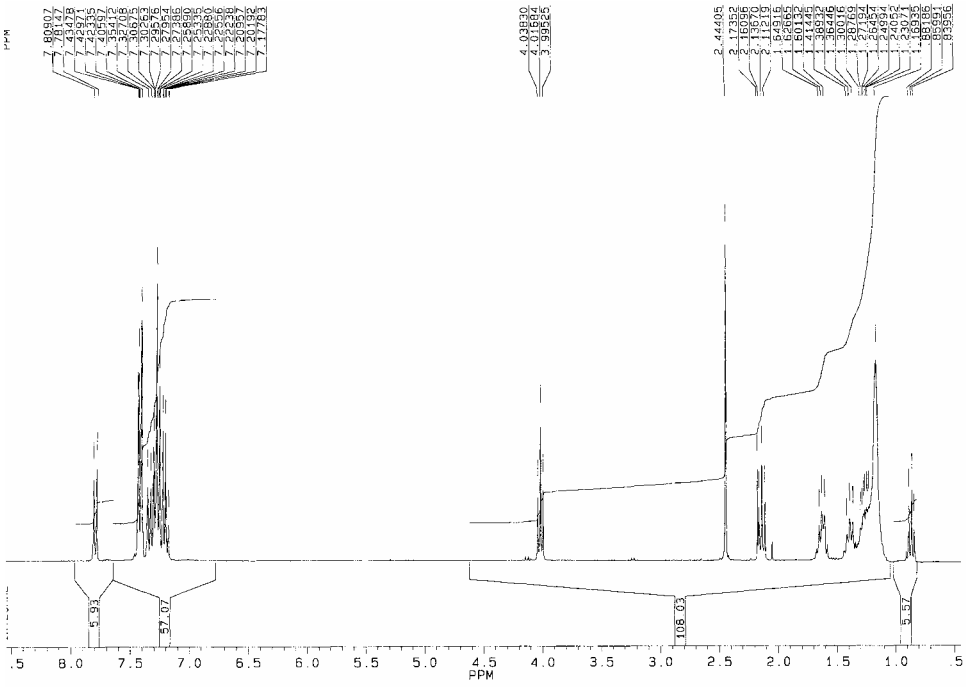

Figure 5.7. ^{1}H NMR spectrum (300 MHz) of **9** in $CDCl_3$

9 was then reacted with **1** to yield **5** in 56% yield. The latter was then converted in the target **8** in three more final steps identical to those described in scheme 5.1 with a 37% overall yield.

5.2.2 Luminescence quenching in supramolecular assemblies of quantum dots and bipyridinium dications

Semiconductor quantum dots (QDs) are inorganic particles with nanoscaled diameters and outstanding photophysical properties.[13] Their spectroscopic signature can be manipulated with fine adjustments in elemental composition and physical dimensions to afford luminescent probes with tunable emissive behavior. Indeed, the modularity of these inorganic nanostructures coupled to intrinsically high absorption cross sections, outstanding photobleaching resistances and long luminescence lifetimes are encouraging their use in biomedical imaging and sensing applications in alternative to conventional organic fluorophores.[14] Specifically, protocols to signal target analytes with luminescent QDs are starting to be developed on the basis of electron and energy transfer processes.[15] In fact, fundamental investigations have demonstrated that these inorganic nanostructures can exchange electrons with complementary organic partners upon excitation with a concomitant

13. a) M. G. Bawendi, M. L. Steigerwald, L. E. Brus, *Ann. Rev. Phys. Chem.*, **1990**, *41*, 477 b) A. P. Alivisatos, *Science*, **1996**, *271*, 933 c) Al. L. Efros ,L. Rosen, *Ann. Rev. Mater. Sci.*, **2000**, *30*, 475 d) A. D. Yoffe, *Adv. Phys.*, **2001**, *50*, 1 e) C. Burda, X. B. Chen, R. Narayana, M. A. El-Sayed, *Chem. Rev.*, **2005**, *105*, 1025

14. a) C. M. Niemeyer, *Angew. Chem. Int. Ed.*, **2003**, *42*, 5796 b) I. Willner, E. Katz, *Angew. Chem. Int. Ed.*, **2004**, *43*, 6042 c) A. P. Alivisatos, *Nature Biotechnol.*, **2004**, *22*, 47 d) N. L. Rosi, C. A. Mirkin, *Chem. Rev.*, **2005**, *105*, 1547 e) X. Gao, L. Yang, J. A. Petros, F. F. Marshall, J. W. Simons, S. Nie, *Curr. Op. Biotechnol.*, **2005**, *16*, 63 f) I. G. Medintz, H. T. Uyeda, E. R. Goldam, H. Mattoussi, *Nature Mater.*, **2005**, *4*, 435 g) X. Michalet, F. F. Pinaud, L. A. Bentolila, J. M. Tsay, S. Doose, J. J. Li, G. Sundaresan, A. M. Wu, S. S. Gambhir, S. Weiss, *Science*, **2005**, *307*, 538

15. a) R. C. Somers, M. G. Bawendi, D. G. Nocera, *Chem. Soc. Rev.*, **2007**, *36*, 579 b) F. M. Raymo, I. Yildiz, *Phys. Chem. Chem. Phys.*, **2007**, *9*, 2036

luminescence quenching.[16] In particular, Raymo et al have exploited the ability of CdSe–ZnS core–shell QDs to inject electrons into bipyridinium dications to develop photochromic materials[16e] and probe protein–ligand interactions.[16h] These strategies are based on the adsorption of appropriate bipyridinium dications on the surface of the inorganic MPCs in the ground state and on the exchange of electrons between them in the excited state. In order to elucidate further the fundamental factors governing these processes and broaden the array of basic building blocks available for the implementation of these strategies, we have prepared QDs coated with either tri-*n*-octylphosphine oxide (TOPO) or a tris(phenylureido)calix[6]arene **8** and investigated the interactions of the resulting assemblies QD–TOPO and QD–**8** with the bipyridinium dications $\mathbf{14}^{2+}$ and $\mathbf{15}^{2+}$ (see Figure 5.8).

We have synthesized QD–TOPO, $\mathbf{14}^{2+}$ and $\mathbf{15}^{2+}$ according to established literature procedures.[17] Specifically, we have reacted CdO and Se at high temperature in the presence of TOPO and then treated the

16. a) M. G. Sandros, D. Gao, D. E. Benson, *J. Am. Chem. Soc.*, **2005**, *127*, 12198 (b) B. P. Aryal and D. E. Benson, *J. Am. Chem. Soc.*, **2006**, *128*, 15986 (c) K. Palaniappan, C. Xue, G. Arumugam, S. A. Hackney, J. Liu, *Chem. Mater.*, **2006**, *18*, 1275 (d) R. Gill, R. Freeman, J.-P. Xu, I. Willner, S. Winograd, I. Shweky, U. Banin, *J. Am. Chem. Soc.*, **2006**, *128*, 15376 (e) I. Yildiz, F. M. Raymo, *J. Mater. Chem.*, **2006**, *16*, 1118 (f) M. Tomasulo, I. Yildiz, F. M. Raymo, *J. Phys. Chem. B*, **2006**, *110*, 3853 (g) M. Tomasulo, I. Yildiz, S. L. Kaanumalle, F. M. Raymo, *Langmuir*, **2006**, *22*, 10284 (h) I. Yildiz, M. Tomasulo, F. M. Raymo, *Proc. Natl. Acad. Sci. USA*, **2006**, *103*, 11457 (i) V. Maruel, M. Laferrière, P. Billone, R. Godin, J. C. Scaiano, *J. Phys. Chem. B*, **2006**, *110*, 16353 (l) S. J. Clarke, C. A. Hollmann, Z. Zhang, D. Suffern, S. E. Bradforth, N. M. Dimitrijevic, W. G. Minarik, J. L. Nadeau, *Nat. Mater.* **2006**, *5*, 409 (m)

17. a) B. O. Dabbousi, J. Rodriguez-Viejo, F. V. Mikulec, J. R. Heine, H. Mattoussi, R. Ober, K. F. Jensen, M. G. Bawendi, *J. Phys. Chem. B*, **1997**, *101*, 9463; b) Z. A. Peng, X. Peng, *J. Am. Chem. Soc.*, **2001**, *123*, 183 c) R. J. Alvarado, J. Mukherjee, E. J. Pacsial, D. Alexander, F. M. Raymo, *J. Phys. Chem. B*, **2005**, *109*, 6164

resulting MPCs with Et_2Zn and hexamethyldisilathiane to generate QD–TOPO.

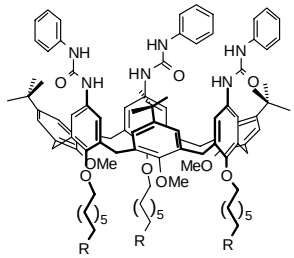

8 R = $CH_2(CH_2)_2CH_2SH$
16 R = CH_3

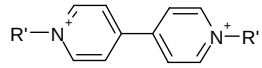

14 R' = $(CH_2)_9CH_3$
15 R' = $(CH_2)_7CH_3$

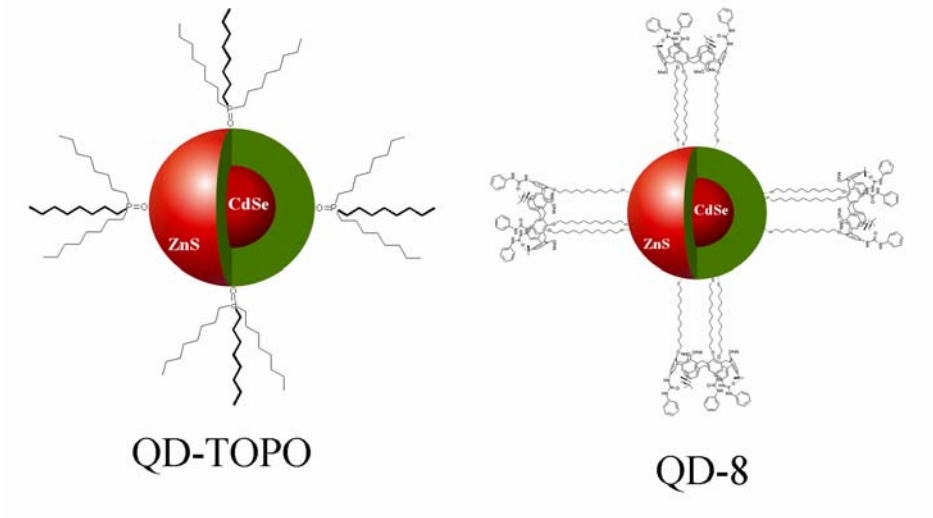

Figure 5.8. The bipyridinium dications $\mathbf{14}^{2+}$ and $\mathbf{15}^{2+}$, the calix[6]arenes **8** and **16** and schematic representations of QD–TOPO and QD–**8** (the parts of the cartoons are not in scale).

Similarly, we have reacted 4,4'-bipyridine with an excess of either decylbromide or octylbromide and then exchanged the bromide counterions of the resulting dications with either hexafluorophosphate or chloride anions to generate **14**·2Cl, **14**·$2PF_6$ and **15**·$2PF_6$. The emission spectrum (Figure 5.9, full line) of a dispersion of QD–TOPO in $CHCl_3$

shows an intense band centered at 547 nm with a luminescence quantum yield of 0.38 and an average luminescence lifetime of 16 ns. This band decreases in intensity (Figure 5.9, dashed lines) with the addition of increasing amounts of either **14**·2Cl or **14**·2PF_6 or even **15**·2PF_6.

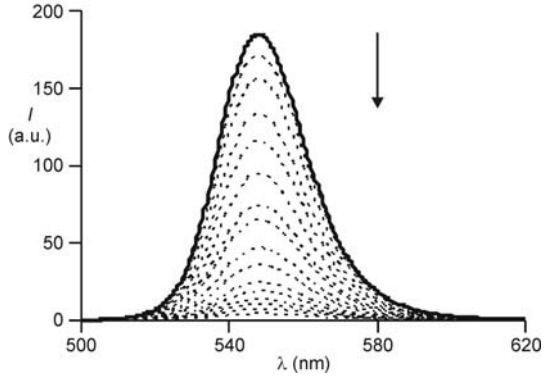

Figure 5.9. Emission spectra of QD–TOPO (0.08 μM, $CHCl_3$, λ_{Ex} = 400 nm) before (–) and after (- - -) the addition of increasing amounts (0–1.5 μM) of **14**·2Cl.

Instead, the presence of either $\mathbf{14}^{2+}$ or $\mathbf{15}^{2+}$ has negligible influence on the absorption spectrum of QD–TOPO (Figure 5.10).

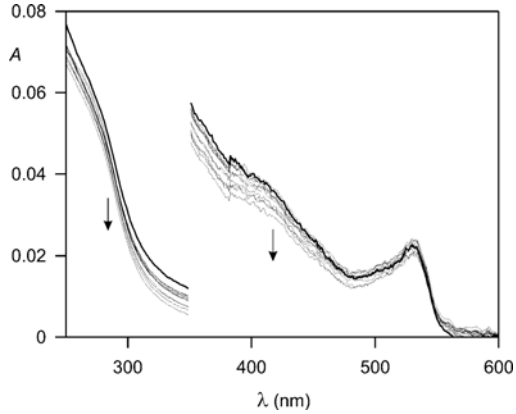

Figure 5.10. Absorption spectra of QD–TOPO (0.08 μM, $CHCl_3$) before (thick line) and after (thin lines) the addition of increasing amounts (0–1.5 μM) of **14**·2Cl. The small absorbance decrease can be ascribed to dilution effects

In all instances, the concentration of the bipyridinium dication has negligible influence on the average luminescence lifetime (***a*** in Figure 5.11), but affects drastically the luminescence intensity (***b*** in Figure 5.11). These observations are consistent with static quenching and demonstrate that the luminescent MPCs and the dicationic quencher associate in the ground state.

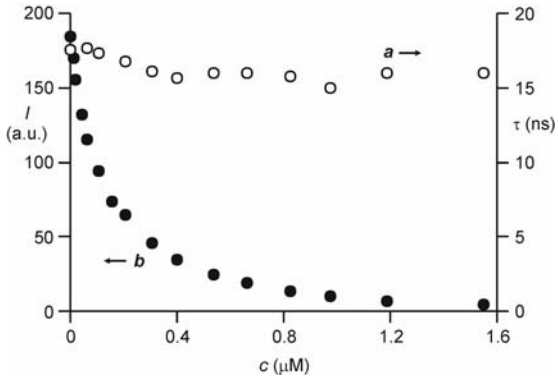

Figure 5.11. Plots of the average luminescence lifetime (*a*, right scale) and luminescence intensity (*b*, left scale) of QD–TOPO (0.08 μM, $CHCl_3$, λ_{Ex} = 400 nm) against the concentration of **14**·2Cl.

The corresponding association constants (K) and quenching rate constants (k_q) are listed in Table 5.1 and were determined from the analysis of the Stern–Volmer plots.

Table 5.1. Association constants (K) for the complexes formed between QD–TOPO and the dicationic quenchers in $CHCl_3$ and the corresponding quenching rate constants (k_q)

	K (M^{-1})	k_q (s^{-1})
14·2Cl	$(1.1 \pm 0.1) \times 10^7$	2.2×10^9
14·2PF_6	$(3.2 \pm 0.3) \times 10^5$	1.7×10^9
15·2PF_6	$(1.7 \pm 0.2) \times 10^5$	2.7×10^8

Figure 5.12 shows the Stern–Volmer plots obtained from luminescence intensity and lifetime measurements upon addition of **14**·2Cl to QD–TOPO. Qualitatively similar results have been obtained with **14**·2PF_6 or **15**·2PF_6 as the quenchers or with QD–**8** as the luminophore. The non-linearity of the Stern–Volmer plot for luminescence intensity and the invariance of the luminescence lifetime on increasing the quencher concentration indicate that the quenching is static in nature, *i.e.*, the QD and bipyridinium dications are associated in their ground state.

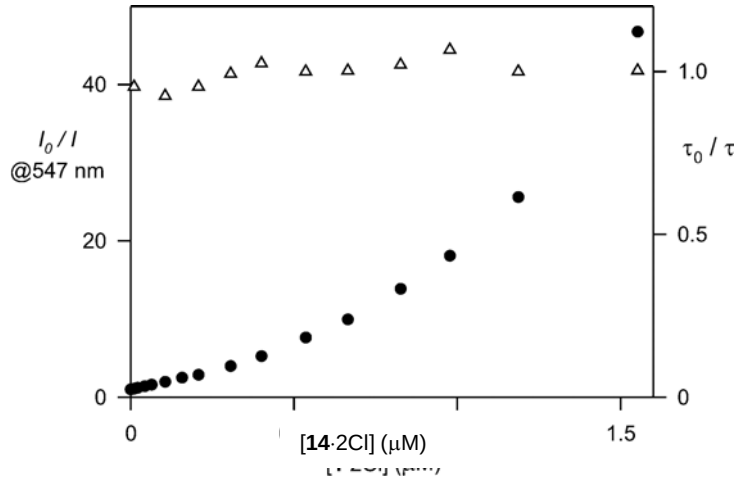

Figure 5.12. Stern–Volmer plots obtained from luminescence intensity (circles; left scale, I_0/I) and lifetime (triangles; right scale, τ_0/τ) measurements upon addition of **14**·2Cl to QD–TOPO in $CHCl_3$.

In case of static quenching the luminescence behavior of the system can be described[18] by means of the following equation:

$$\frac{I_0}{I} = 1 + \left(k_q \tau_0 + K \frac{\varepsilon_{L.Q}}{\varepsilon_L} \right) [Q] + k_q \tau_0 K \frac{\varepsilon_{L.Q}}{\varepsilon_L} [Q]^2 \qquad \text{(eq. 1)}$$

18. V. Balzani, L. Moggi, M. F. Manfrin, F. Bolletta, G. S. Laurence, *Coord. Chem. Rev.*, **1975**, *15*, 321

wherein: I_0 and I are the luminescence intensity of the luminophore in the absence and in the presence of the quencher, respectively; τ_0 is the luminescence lifetime of the luminophore in the absence of quencher; k_q is the bimolecular (dynamic) quenching rate constant; K is the stability constant of the luminophore-quencher complex; [Q] is the molar concentration of the quencher; and ε_L and $\varepsilon_{L.Q}$ are the molar absorption coefficients of the luminophore and of the luminophore–quencher complex, respectively, at the excitation wavelength (in this case $\varepsilon_{L.Q}/\varepsilon_L \approx 0.8$ at 400 nm, see Figure 5.13).

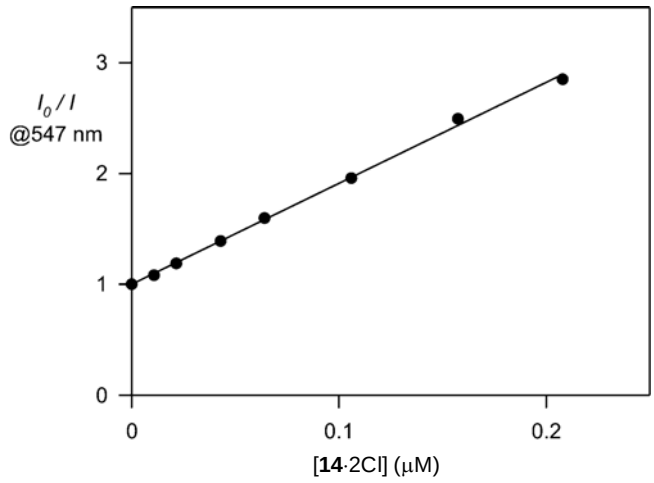

Figure 5.13. Stern–Volmer plot obtained from luminescence intensity measurements (I_0/I) upon addition of up to 2.0 mM of **14**·2Cl to QD–TOPO in $CHCl_3$. The line represents the fitting to the data points according to eq. (1).

Since in our case $K\varepsilon_{L.Q}/\varepsilon_L$ is certainly much larger than $k_q\tau_0$, at small quencher concentrations the third term of the equation can be neglected and a linear Stern–Volmer plot, whose slope is equal to $[k_q\tau_0 + K\varepsilon_{L.Q}/\varepsilon_L] \approx K\varepsilon_{L.Q}/\varepsilon_L$, is obtained. As a matter of fact, the first part of the Stern–Volmer plot can be satisfactorily fitted by a linear regression (Figure 5.13),

yielding a slope of 9.1 μM^{-1} and an association constant of 11.4 μM^{-1}. The same value, within experimental error, is obtained by fitting the luminescence spectral changes with the Specfit software[19] by assuming a 1:1 binding model.The quenching rate constant was estimated from equation (2),

$$k_q = 1/\tau_0 \, (I_0/I - 1) \qquad \text{(eq. 2)}$$

where τ_0 and I_0 are the luminescence lifetime and intensity of the luminophore in the absence of the quencher, respectively, and I is the luminescence intensity observed for the luminophore-quencher complex (taken as that corresponding to the plateau at end of the titration). For example, in the case of the QD–TOPO/**14**·2Cl pair,

$$k_q = 1/(16\times10^{-9}) \times (180/5 - 1) = 2.2 \times 10^9 \ s^{-1} \qquad \text{(eq. 3)}$$

The above described analysis of the Stern–Volmer plot was applied to all the examined luminophore–quencher pairs

A comparison of the data in Table 5.1 indicates that K increases by two orders of magnitude with the transition from hexafluorophosphate to chloride counterions and by *ca.* 50% with the elongation of the alkyl substituents from octyl to decyl chains. The former observation can be ascribed to a stronger solvophobic effect experienced by **14**·2Cl compared to **14**·2PF_6, as reflected by the solubilities of these salts in chloroform. On the contrary, the type of counterion of the quencher has little effect on the quenching rate constant, which however drops by one

19. R. A. Binstead, SPECFIT, Spectrum Software Associates, Chapel Hill, NC, **1996**

order of magnitude upon replacing the decyl side chains with octyl ones. In agreement with literature data,[20] electron transfer from the excited MPCs to either $\mathbf{14}^{2+}$ or $\mathbf{15}^{2+}$ is, presumably, responsible for quenching. Nonetheless, the characteristic spectroscopic signature of the radical cation of either $\mathbf{14}^{2+}$ or $\mathbf{15}^{2+}$ cannot be observed by nanosecond flash photolysis measurements, suggesting that back electron transfer occurs on a subnanosecond timescale. Since the redox properties of bipyridinium dications are nearly unaffected[8d] by the type of alkyl substituent present on the nitrogen atoms, one can infer that the difference in the quenching rate constant between $\mathbf{14}^{2+}$ and $\mathbf{15}^{2+}$ is related to the fact that the former can reach closer to the QD surface compared to the latter.

The treatment of QD–TOPO with **8** results in the adsorption of the macrocyclic receptor on the surface of the MPCs. As a result, the luminescence intensity decreases by 30% with a bathochromic shift of 5 nm and the average luminescence lifetime drops to 9 ns. After the addition of increasing amounts of either **14**·2Cl or **14**·$2PF_6$ or even **15**·$2PF_6$, a broad and weak band extending up to 600 nm appears in the absorption spectrum (Figure 5.14). Presumably, this absorption arises from charge-transfer interactions between the electron rich calixarene and the electron deficient dications.[8d]

20. a) S. Logunov, T. Green, S. Marguet, M. A. El- Sayed, *J. Phys. Chem. A*, **1998**, *102*, 5652 b) C. Burda, T. C. Green, S. Link, M. A. El-Sayed, *J. Phys. Chem. B*, **1999**, *103*, 1783

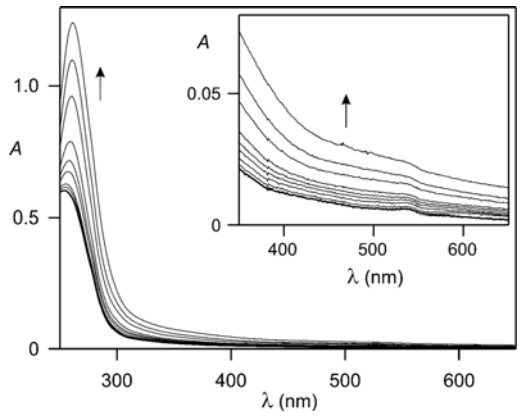

Figure 5.14. Absorption spectra of QD–**8** (0.12 μM, $CHCl_3$) before (thick line) and after (thin line) the addition of increasing amounts (0–50 μM) of **14**·2Cl. The inset shows a magnification of the region comprised between 350 and 650 nm

Once again, the luminescence intensity QDs decreases with the concentration of the bipyridinium dications, while the average luminescence lifetime remains essentially unaffected. This behavior is consistent with static quenching and confirms the formation of ground-state complexes between the luminescent MPCs and the dications quenchers. The corresponding K and k_q are listed in Table 5.2 and were determined from the analysis of the Stern–Volmer plots.

Table 5.2. Association constants (K) for the complexes formed between QD–**8** and the dicationic quenchers in $CHCl_3$ and the corresponding quenching rate constants (k_q)

	K (M^{-1})	k_q (s^{-1})
14·2Cl	$(1.0 \pm 0.1) \times 10^5$	5.4×10^8
14·2PF_6	$(2.4 \pm 0.4) \times 10^4$	1.2×10^8
15·2PF_6	$(1.0 \pm 0.1) \times 10^4$	2.0×10^8

A comparison of the data in Table 5.2 indicates that K increases by one order of magnitude with the transition from hexafluorophosphate to

chloride counterions and by *ca.* 50% with the elongation of the alkyl substituents from octyl to decyl chains. Interestingly, the nature of ligands on the surface of the MPCs has a pronounced influence on *K*. Specifically, the bipyridinium complexes of QD–TOPO are significantly more stable than those of QD–**8**. This trend is in apparent contradiction with the known ability of calixarenes to encapsulate bipyridinium dications in non polar solvents with high association constants.[8d] Presumably, the confinement of **8** on the surface of the inorganic MPCs hinders the insertion of either $\mathbf{14}^{2+}$ or $\mathbf{15}^{2+}$ in its cavity. Chloride anions may favor the association between QD–**8** and $\mathbf{14}^{2+}$ because they can form hydrogen bonds with the ureidic units of **8**.[8d]

The k_q values are one order of magnitude smaller than those measured for QD–TOPO. These observations can be rationalized considering that the inclusion of $\mathbf{14}^{2+}$ or $\mathbf{15}^{2+}$ into **8** is expected to have two main consequences. First, their bipyridinium units are kept separated from the QD surface by the monolayer formed by the undecanethiol-derivatized calixarene; second, they become more difficult to reduce, thereby decreasing the driving force for the electron-transfer process.[8d]

The calixarene **16** (Figure 5.8) binds bipyridinium dications in non polar solvents with association constants of *ca.* 10^6 M^{-1}.[8d] As a result, this macrocyclic receptor can compete with QD–TOPO and capture either one of the three bipyridinium quenchers **14**·2Cl, **14**·$2PF_6$ or **15**·$2PF_6$. For example, the luminescence intensity of QD–TOPO (***a*** in Figure 5.15) is almost completely suppressed in the presence of *ca.* 19 equivalents of **14**·2Cl (***b*** in Figure 5.15). However, the original

luminescence intensity is fully restored after the addition of an excess of **16** (***c*** in Figure 5.15). Indeed, the supramolecular association of **16** and $\mathbf{14}^{2+}$ prevents the interaction of the latter with QD–TOPO and supresses the photoinduced electron transfer process. Consistently, this supramolecular event is transduced into a pronounced enhancement in luminescence. Thus, these operating principles can, in principle, be exploited to probe receptor–substrate interactions with luminescence measurements

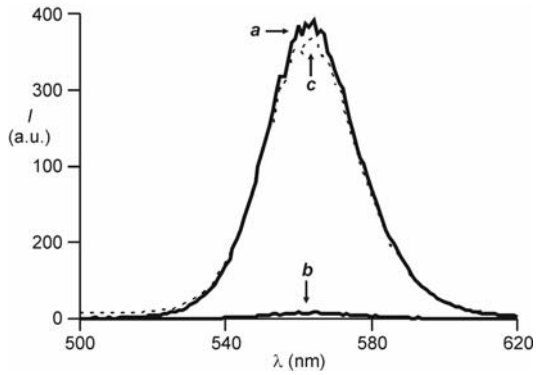

Figure 5.15. Emission spectra of QD–TOPO (0.43 μM, $CHCl_3$, λ_{Ex} = 350 nm) before (*a*) and after the sequential addition of **14**·2Cl (*b*, 8.0 μM) and **16** (*c*, 160 μM)

These results demonstrate that bipyridinium dications associate with either QD–TOPO or QD–**8** in the ground state with *K* ranging from 10^4 to 10^7 M^{-1} in $CHCl_3$. The counterions of the bipyridinium dications as well as the ligands on the surface of the QDs control the stability of the resulting complexes. The length of the aliphatic chains appended to the bipyridinium core has a minor influence on the binding event. In these supramolecular assemblies, the bipyridinium dications quench the luminescence of the MPCs with k_q ranging from 10^8 to 10^9 s^{-1}, presumably by photoinduced electron transfer from the inorganic core.

Interestingly, the transition from TOPO to **8** ligands has a depressive effect on the stability of the bipyridinium complexes and delays the quenching process significantly. In the presence of **16**, the bipyridinium quenchers desorb from the surface of QD–TOPO and associate with the calixarene instead. As a result, the original luminescence intensity of the MPCs is restored. Thus, the supramolecular association of the quencher with a complementary receptor can be transduced into a luminescence enhancement with these operating principles.

5.2.3 Preparation of calix[6]arene-based rotaxanes supported on Au MPCs

In the last part of the PhD thesis, starting from the promising results in the preparation of calix[6]arene-coated CdSe clusters, we explored the possibility to stabilize Au MPCs with calix[6]arene **8** with the aim to study the electrochemical properties of rotaxane-based structures supported on Au surface. The **8**-stabilized Au clusters were prepared by "place-ligand exchanges reaction" starting from Au MPCs stabilized with TOABr as seen in Chapter 4. The resulting clusters experienced very low solubility in common low polar solvents like toluene, chloroform and dichloromethane. As matter of fact, the **8**-stabilized Au MPCs were separated through filtration from the reaction media (toluene). Such clusters could be, however, easily dissolved in the more polar acetone. This behaviour was in contrast with the solubility properties showed by the calix[4]arene-coated Au MPCs (see Chapters 3 and 4) and it was ascribed to the presence of the phenylureido moieties in the macrocycle.

These functions might induce a certain degree of aggregation of the clusters due to intramolecular hydrogen bonding exerted by the urea groups.

A qualitative evaluation of the aggregation phenomenon was obtained using as usual UV-Vis spectroscopy. In Figure 5.16 have been reported the optical spectra acetone for the TOABr-stabilized (black line) and **8**-stabilized (red line) Au MPCs, respectively. The surface plasmon band (SPB) of the latter clusters is shifted at higher wavelength, thus indicating that larger clusters were present in solution.

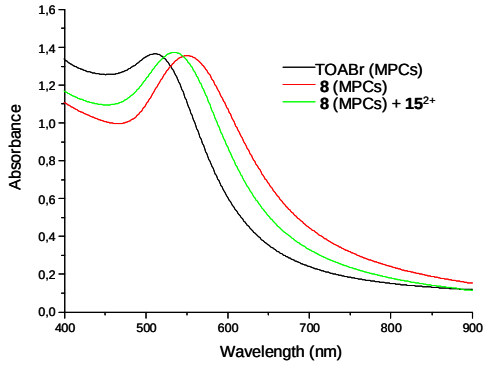

Figure 5.16. UV-Vis spectra in acetone of Au MPCs stabilized with TOABr (black line), with calix[6]arene **8** (red line), and with **8** after the addition of **15**$^{2+}$(green line), respectively.

The red-shift of the SPB of **8** Au MPCs was effectively due to the aggregation between the calix[6]arene units present onto the clusters surfaces. Indeed, the addition of a small amount of the dioctylviolgen salt **15** 2Ts (see Figure 5.8) to the solution containing the aggregated clusters, determined a blu shift of the SPB (see Figure 5.16, green line). On the other hand it has been demonstrated that the cavity of **8** is able to

recognize viologen salts such as **15** 2Ts giving rise to very stable pseudorotaxane compounds.[8a,d]

These preliminary and qualitative UV-Vis experiments thus supported the hypothesis that formation of pseudorotaxane structures can also occur with the calix[6]arene hosts supported onto the gold surface. On the other hand, it has been previously shown that is possible to control the threading process of a calix[6]arene wheel with monostoppered viologen-based axle simply changing the polarity of the solvent to yield oriented rotaxanes.[10] (see also introduction of this chapter). Our idea was thus to exploit the core of the gold clusters as stopper to form oriented and unoriented rotaxanes onto the gold surface (see Figure 5.17).

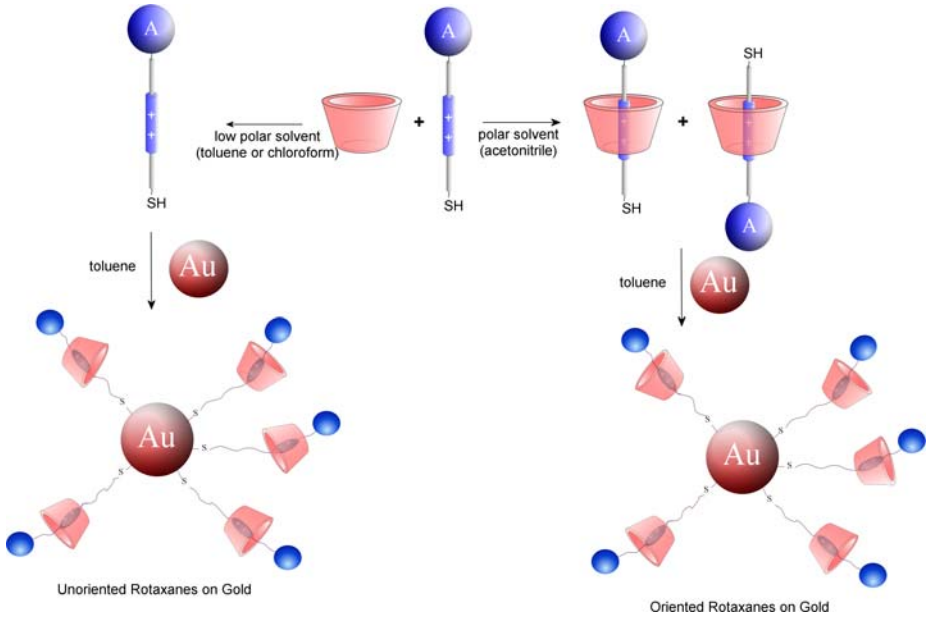

Figure 5.17. Schematic representation of the formation of Oriented and Unoriented Rotaxanes on Au MPCs

To this aim is however necessary to design a viologen-based axle, such as **23** (see Scheme 5.3) stoppered at one of its termini with a bulky group and having on the other termini a thiol group that can be used as anchoring point for the gold surface. We chose as stopper for the thiolated axle the 2,5-di-*tert*-butyl phenol. This group is enough bulkier to prevent the full threading of the axle within the calix[6]arene cavity. The synthesis of **23** was summarized in scheme 5.3.

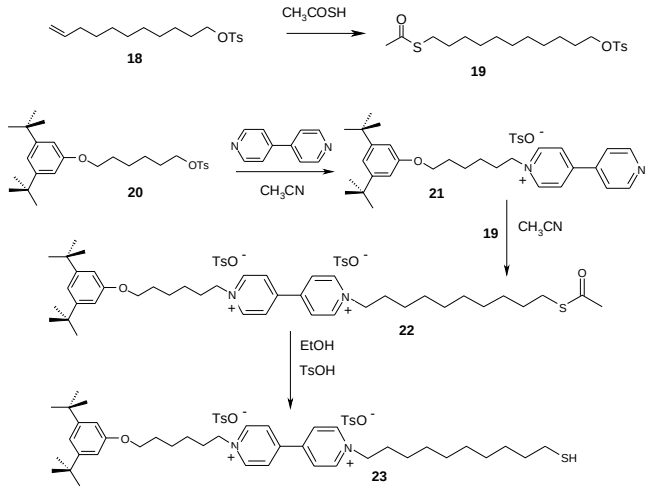

Scheme 5. 3. Synthesis of thiolated axle **23**

The known tosylate **20** was used to alkylate the 4,4'-bipyridile to afford the monoalkylated salt **21**·Ts. **21** was then converted in the axle **22** in which the thiol group is still protected as thioacetyl. Removal of the thioacetyl PG final afforded the thiolated axle **23** in 70% yield. From the ^{1}H-NMR is possible to notice all characteristic signals of an asymmetric 4,4'-bipyridinium compound. At 9.19 and 8.79 ppm is possible to see the signals of the bipyridinium unit, in particular the signal at 9.19 is not a doublet but a more complicated signals due to the asymmetry of

compound **23**. The signals of the stoppers are visible at 6.99 and 6.71 ppm. Diagnostic is the presence of the quadruplet at 2.59 ppm due to the CH_2 in α position of the thiol group.

These Au NPs were then used as starting material for the preparation of the "functional" NPs. Initially we prepared a sample of "oriented" pseudorotaxane through a selective threading process in toluene between the monostoppered "axle" **23** and the calix[6]arene wheel **24** (see Scheme **5.9**).[21]

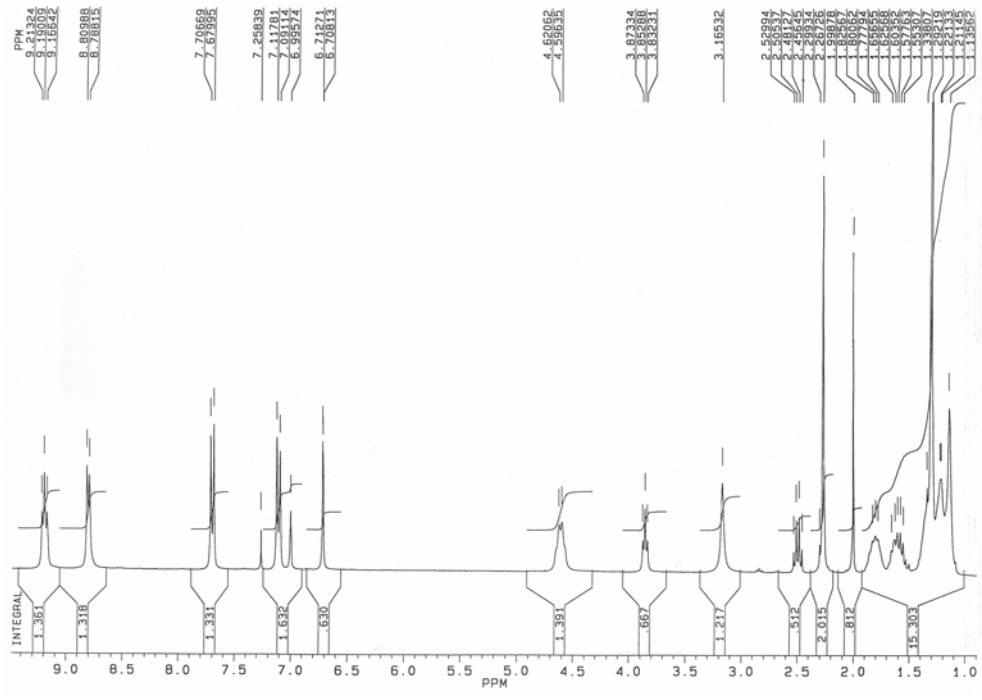

Figure 5.18 ^{1}H-NMR of compound **23** in $CDCl_3$

21. For the synthesis of wheel 24 see Reference 8b

In toluene, the directionality of the threading process is known and the axle threads the wheel from the upper rim of the macrocycle. In contrast, a sample containing the mixture of the two pseudorotaxane isomers was obtaining repeating the threading process in the more polar CH_3CN. We have recorded several NMR spectra to determine the composition of the two samples and we are sure of their identity[22].

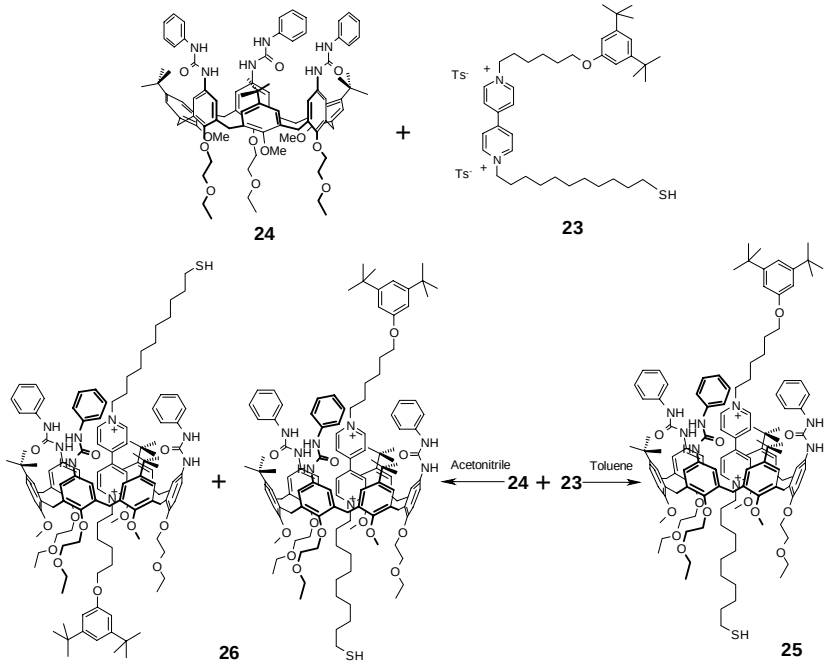

Scheme 5.9 Synthesis of oriented rotaxanes **25** and isomers **26**

The samples containing the "oriented" pseudorotaxanes and the "unoriented" pseudorotaxane mixture were hence used for the exchange reaction in toluene with the Au NPs previously synthesized. (see Figure 5.19)

22 D. Demuru, University of Parma PhD thesis

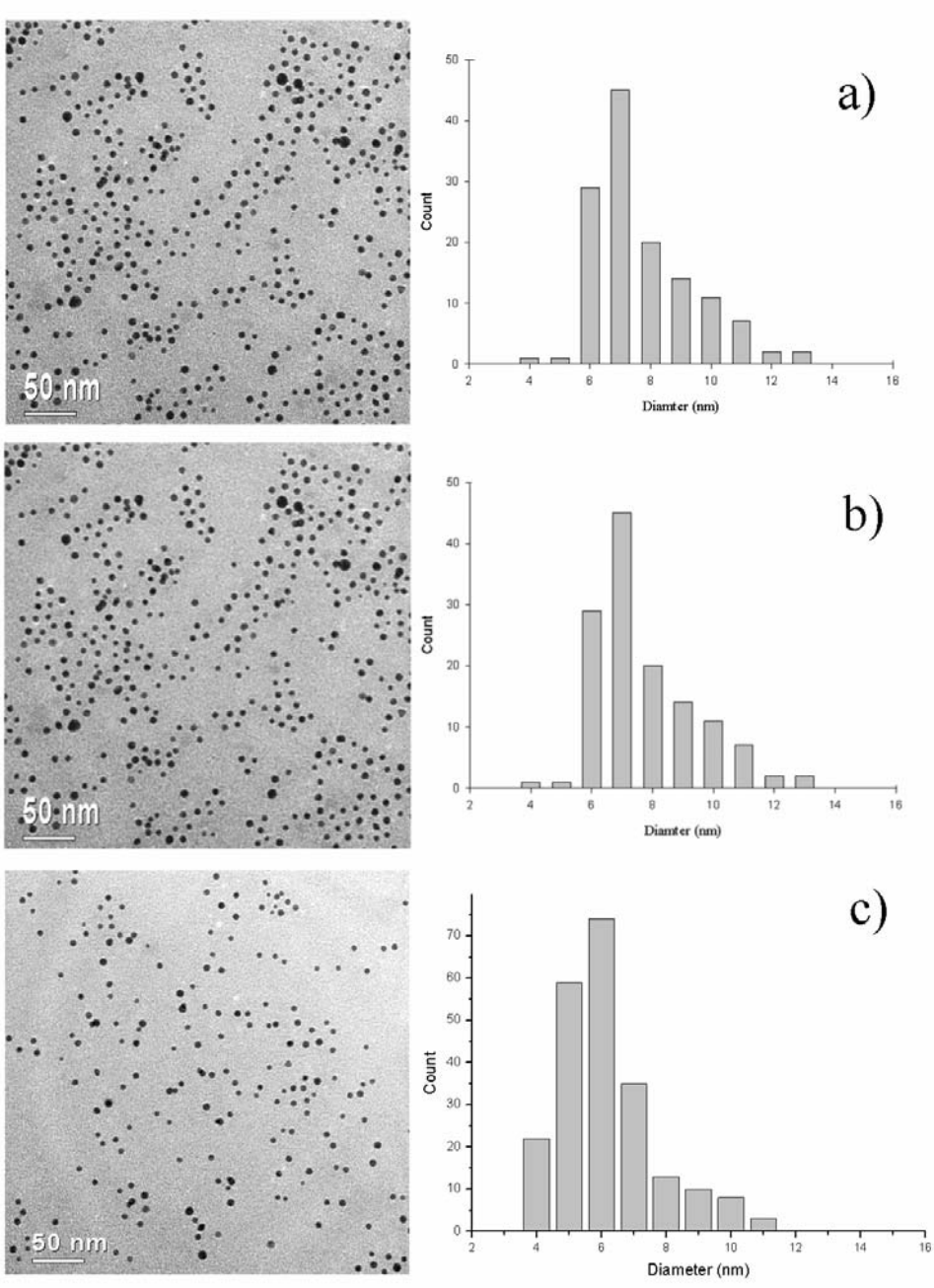

Figure 5.19 Tem images of AuMPCs stabilized by oriented rotaxanes **25** (a), isomers **26** (b) and free axle **23** (c).

Au NPs stabilized only by axle **23** were synthesized just for reference and now the voltammetric measurements and all experiments for the understanding of the properties of these compounds are under investigation in our laboratory.

Experimental Section

General Remarks:

All reactions were carried out under nitrogen, and all solvents were freshly distilled under nitrogen prior to use. All other reagents were reagent grade quality obtained from commercial supplies and used without further purification. Thin-layer chromatography was performed on aluminium sheets coated with silica gel 60F (Mercj 5554). Column chromatography was carried out by using silica gel (ICN 4663, 63-200 mesh). ^{1}H NMR spectra were recorded at 300 MHz. ^{13}C NMR spectra were recorded at 75 MHz. Mass spectra were recorded in the ESI mode.

Synthesis of **2 :** calix[6]arene **1** (1.5 g, 1.5 mmol) and undecenetosilate (1.7 g, 5.4 mmol) were dissolved in 500 ml of acetonitrile. K_2CO_3 (0.8 g, 5.4 mmol) was added and the resulting heterogeneous mixture was refluxed for 7 days. After this period HCl (300 ml 10% in water) and ethyl acetate (100 ml) were added. The organic phase was separated, dried on Na_2SO_4 and concentrated under reduced pressure. The crude product was purified by column cromathography (eluent : hexane / ethyl acetate = 95 /5) obtaining calix[6]arene **3** as a yellowish solid (yield 69%).^{1}H – NMR (300 MHz, $CDCl_3$) δ 7.67 (bs, 6H), 7.21 (bs, 6H), 5.9-5.7 (m, 3H), 5.0-4.9 (m, 6H), 4.6-4.1 (m, 6H), 3.83 (bs, 6H), 3.7-3.4 (m, 6H), 2.86 (s, 9H), 2.1-2.0 (m, 6H), 1.85 (bs, 6H), 1.6-1.0 (m, 53H). ^{13}C – NMR (75MHz, $CDCl_3$) : 146.8, 143.6, 139.1, 127.8, 127.3, 123.1, 114.1,

77.4, 73.9, 59.9, 34.2, 33.7, 31.4, 31.2, 30.9, 30.5, 30.2, 29.4, 29.2, 29.0, 28.8, 26.0.
m.p. 138-140 °C. ESI-MS : 1461.68 [M+Na^+]

Synthesis of **3 :** calix[6]arene **2** (1.3 g, 0.9 mmol) and thioacetic acid (0.2g, 2.8mmol) were dissolved in 100 ml of dry toluene. AIBN is added (catalytic amount) and the mixture refluxed for 12h. After this period distilled water (300 ml) was added. The organic phase collected and concentrated under reduced pressure. Pure **3** was obtained by column chromatography (eluent: hexane / THF = 9 / 1) as a yellowish solid (yield 83%).^{1}H – NMR (300 MHz, $CDCl_3$) δ 7.68 (bs, 6H), 7.23 (bs, 6H), 4.6-4.1 (m, 6H), 3.83 (bs, 6H), 3.7-3.4 (m, 6H), 2.9-2.8 (m, 15H), 2.3 (s, 9H), 1.85 (bs, 6H), 1.7-1.0 (m, 53H). ^{13}C – NMR (75MHz, $CDCl_3$) : 195.8, 159.8; 154.2; 146.7; 143.5, 135.7, 132.1, 129.7, 127.8, 127.3, 123.1, 73.9, 59.8, 34.2, 31.4, 30.9, 30.5, 30.2, 29.4, 29.0, 28.7, 26.8, 26.0, 23.3.
m.p. 146-148 °C. ESI-MS : 1686.66 [M+Na^+]

Synthesis of **4 :** calix[6]arene **3** (1g, 0.6 mmol) was dissolved in THF (50 ml) and HCl (50 ml 10% in water) and the resulting homogeneous mixture refluxed for 3 days. After this period ethyl acetate (20 ml) was added. The organic phase was separated, dried on Na_2SO_4 and concentrated under reduced pressure to obtain compound **4**, which has been used for the next reaction without any other purification.

Synthesis of **5 :** calix[6]arene **4** (0.6g, 0.4 mmol), trityl chloride (0.5g, 1.8 mmol) and triethylammine (0.2g, 2mmol) were dissolved in

acetonitrile (50 ml) and refluxed for 12 h. After this period the solvent was removed and the residue dissolved in ethyl acetate (100 ml). The organic phase was washed twice with HCl (100 ml 10% in water), dried on Na_2SO_4 and concentrated under reduced pressure. Compound **5** was purified by column chromatography (eluent : hexan / ethyl acetate = 9 / 1) as a yellowish solid (yield 77%).^{1}H – NMR (300 MHz, $CDCl_3$) δ 7.67 (bs, 6H), 7.6-7.1 (m, 51H), 4.6-4.1 (m, 6H), 3.81 (bs, 6H), 3.7- 3.4 (bs, 6H), 2.85 (s, 9H), 2.12 (t, 6H, *J* = 7.3 Hz), 1.83 (bs, 6H), 1.8-1.0 (m, 53H). ^{13}C – NMR (75MHz, $CDCl_3$) : 146.8, 145.1, 132.1, 129.9, 129.6, 129.5, 129.3, 128.9, 128.7, 128.3, 128.2, 127.9, 127.7, 127.6, 127.4, 127.3, 127.2, 126.6, 126.4, 126.3, 123.1, 115.3, 73.9, 66.33, 34.2, 32.0, 31.4, 30.2, 29.7, 29.5, 29.4, 29.2, 29.0, 28.6, 25.0.
m.p. 100-103 °C. ESI-MS : 2288.66 [M+Na^+]

Synthesis of **6 :** in a 250 ml two neck round bottom flask calix[6]arene **5** (0.58g, 0.26 mmol) was suspended in n-butanol (150 ml). Under nitrogen Pd on activated charcoal (catalytic amount) was added. The mixture was stirred for few minutes and than hydrazin monohydrate (0.64g, 13 mmol) was added. The resulting heterogeneous mixture was refluxed for 12 h. The crude of the reaction was cooled at room temperature and the Pd/C removed by filtration on celite maintaining the equipment under N_2 atmosphere. The solvent was removed under reduced pressure and the triammine calix[6]arene **6** was used for the next reaction without any other purification.

Synthesis of **7 :** calix[6]arene **6** (0.55g, 0.25mmol) and phenylisocianate (0.15g, 1.26 mmol) were dissolved in CH_2Cl_2 (100 ml) dry and stirred at room temperature for 4 h. The organic solvent was removed under reduced pressure and the crude compound **7** was triturated in methanol to obtain calix[6]arene as a pale yellow solid (yield 84%).^{1}H – NMR (300 MHz, $CDCl_3$) δ 7.7-6.8 (m, 72H), 6.30 (s, 6H), 4.38 (d, 6H, *J* = 15.1 Hz), 3.89 (bt, 6H), 3.54 (d, 6H, *J* = 15.4 Hz), 2.82 (bs, 9H), 2.13 (t, 6H, *J* = 7.2 Hz), 1.87 (bs, 6H), 1.55 (bs, 6H), 1.5-1.0 (m, 47H). ^{13}C – NMR (75MHz, $CDCl_3$) : 154.9, 154.4, 152.0, 146.8, 145.0, 138.0, 135.5, 132.9, 132.3, 129.5, 128.8, 128.2, 127.8, 127.7, 127.2, 126.4, 123.4, 122.5, 120.5, 73.1, 66.3, 60.2, 34.2, 32.0, 31.5, 30.9, 30.5, 29.5, 29.3, 29.1, 28.9, 28.5, 26.2.
m.p. 128-130 °C. ESI-MS : 2557.23 [M+Na^+]

Synthesis of **8 :** calix[6]arene **7** (0.05g, 0.02 mmol) was dissolved in CH_2Cl_2 (20 ml) and TFA (10 ml). $NaBH_3CN$ (0.006g, 0.1 mmol) was added and the mixture stirred at room temperature for 3 h. Water (30 ml) was added and the organic phase collected, dried on Na_2SO_4 and concentrated under reduced pressure. The crude product was triturated in methanol to obtain calix[6]arene **8** as a pale yellow solid (yield 86%).^{1}H – NMR (300 MHz, $CDCl_3$) δ 7.4- 6.8 (m, 27H), 6.27 (s, 6H), 4.38 (d, 6H, *J* = 15.4 Hz), 3.90 (t, 6H, *J* = 6.0 Hz), 3.55 (d, 6H, *J* = 15.6 Hz), 2.82 (bs, 9H), 2.51 (q, 6H, *J* = 7.2 Hz), 1.88 (t, 6H, *J* = 6.8 Hz), 1.8-1.0 (m, 53H). ^{13}C – NMR (75MHz, $CDCl_3$) :154.9, 154.5, 152.3, 146.7, 138.2, 135.7, 133.0, 132.3, 129.4, 129.3, 128.8, 128.7, 128.20, 127.6, 126.2, 123.4,

123.1, 120.5, 73.0, 60.2, 34.1, 34.0, 31.8, 31.5, 31.0, 30.5, 29.6, 29.5, 29.4, 29.3, 29.2, 29.0, 28.8, 28.3, 26.2, 24.6.
m.p. 137-142 °C. ESI-MS : 1830.6 [M+Na^+]

Synthesis of 11-tritil-1-undecanol **:** 11-bromide-1-undecanol (0.5g, 1.9 mmol), tritylthiol (0.55g, 1.9 mmol) and K_2CO_3 (0.27g, 1.9 mmol) were suspended in acetonitrile (50 ml) and refluxed for 4h. Distilled water (20 ml) was added. The organic phase was collected, dried on Na_2SO_4 and concentrated under reduced pressure. The pure compound was obtained after chromatography purification (hexane / ethyl acetate = 8 / 2) as a yellowish oil. (yield 97%)
^{1}H-NMR (300 MHz, $CDCl_3$) δ 7.5-7.0 (m, 15H, Ar**H**), 3.63 (t, 2H, *J* = 6.6 Hz, HOC**H$_2$**), 2.13 (t, 2H, *J* = 7.2 Hz, SC**H$_2$**), 1.6-1.0 (m, 18H, C**H$_2$**).^{13}C-NMR (75 MHz, $CDCl_3$) δ 145.1, 130.1, 129.6, 128.7, 127.9, 127.7, 127.3, 126.8, 126.7, 126.4, 66.3, 63.0, 32.8, 32.7, 32.0, 30.0, 29.5, 29.4, 29.3, 29.2, 29.1, 29.0, 29.0, 28.8, 28.7, 28.6, 28.5, 28.1, 25.7.
ESI-MS 469.2 (M+Na^+)

Synthesis of **9 :** 11-tritil-1-undecanol (0.7g, 1.5 mmol), methylsulfonylchloride (0.3g, 1.5mmol), trietyhlammine (0.4g, 4.5 mmol) and DMAP were dissolved in dry CH_2Cl_2 (100 ml) and stirred at room temperature for 12h. Distilled water (50 ml) was added. The organic phase was collected, dried on Na_2SO_4 and concentrated under reduced pressure. Pure **9** was obtained after chromatography purification (hexane / ethyl acetate = 8 / 2) as a yellowish oil. (yield 90%)

^{1}H-NMR (300 MHz, $CDCl_3$) δ 7.79 (d, 2H, *J* = 8.3 Hz, Ar**H**) 7.5-7.1 (m, 17H, Ar**H**), 4.02 (t, 2H, *J* = 6.5 Hz, $SO_3C\mathbf{H_2}$), 2.44 (s, 3H, $ArC\mathbf{H_3}$) 2.14 (t, 2H, *J* = 7.2 Hz, $SC\mathbf{H_2}$), 1.63 (q, 2H, *J* = 6.8 Hz, $SO_3CH_2C\mathbf{H_2}$) 1.5-1.1 (m, 16H, $C\mathbf{H_2}$).^{13}C-NMR (75 MHz, $CDCl_3$) δ 145.0, 145.5, 133.2, 129.7, 129.5, 129.2, 127.8, 127.7, 126.4, 70.6, 66.3, 32.0, 29.3, 29.3, 29.1, 28.9, 28.8, 28.7, 28.5, 25.3, 22.6, 21.6.
ESI-MS 623.3 ($M+Na^+$)

Synthesis of **5 : 1** (1.5g, 1.5 mmol), **9** (3.2g, 5.3 mmol) and K_2CO_3 (0.7g, 5.0 mmol) were suspended in acetonitrile (200 ml) and refluxed for 10 days. After this period HCl (300 ml 10% in water) and ethyl acetate (100 ml) were added. The organic phase was separated, dried on Na_2SO_4 and concentrated under reduced pressure. The crude product was purified by column cromathography (eluent : hexane / ethyl acetate = 95 /5) obtaining **8** as a yellowish solid (yield 54%).
^{1}H – NMR (300 MHz, $CDCl_3$) δ 7.67 (bs, 6H, Ar**H**), 7.6-7.1 (m, 51H, Ar**H**), 4.6-4.1 (m, 6H, H_{ax} of $ArC\mathbf{H_2}Ar$), 3.81 (bs, 6H, $OC\mathbf{H_2}$), 3.7- 3.4 (bs, 6H, H_{eq} of $ArC\mathbf{H_2}Ar$), 2.85 (s, 9H, $OC\mathbf{H_3}$), 2.12 (t, 6H, *J* = 7.3 Hz, $SC\mathbf{H_2}$), 1.83 (bs, 6H, $OCH_2C\mathbf{H_2}$), 1.8-1.0 (m, 53H, $CH_2C\mathbf{H_2}CH_2$). ^{13}C – NMR (75MHz, $CDCl_3$) : 146.8, 145.1, 132.1, 129.9, 129.6, 129.5, 129.3, 128.9, 128.7, 128.3, 128.2, 127.9, 127.7, 127.6, 127.4, 127.3, 127.2, 126.6, 126.4, 126.3, 123.1, 115.3, 73.9, 66.33, 34.2, 32.0, 31.4, 30.2, 29.7, 29.5, 29.4, 29.2, 29.0, 28.6, 25.0.
m.p. 100-103 °C. ESI-MS : 2288.66 [$M+Na^+$]

Synthesis of **19:** Toluene-4-sulfonic acid undec-10-enyl ester (18) (5.0 g, 15.4 mmol) and thioacetic acid (2.3 g, 31.0 mmol) were dissolved in toluene (200 ml). The resulting solution was degassed with argon for 30 min., then a catalytic amount of AIBN (catalytic amount) was added. After refluxing the solution for 3 h, the solvent was completely evaporated under vacuum, the solid residue was taken up with CH_2Cl_2 and H_2O. The separated organic layer was then washed with a saturated solution of $NaHCO_3$, dried over Na_2SO_4, and evaporated to dryness. Purification of the residue by column chromatography (silica gel, hexane 90%-ethyl acetate 10%) yields a yellow viscous solid (90%). **^{1}H NMR** ($CDCl_3$, 300 MHz, ppm): δ 1.2-1.3(14H, m), 1.5-1.7(4H, m), 2.32(3H, s), 2.45(3H, s), 2.85(2H, J=6 Hz, t), 4.00(2H, J=6 Hz, t), 7.32(2H, J=8 Hz, t), 7.78(2H, J=8 Hz, d). **^{13}C NMR** ($CDCl_3$, 75 MHz, ppm): δ 22.0, 25.7, 29.2, 29.3, 29.4, 29.5, 29.6, 29.7, 29.9, 31.1, 71.1, 128.3, 130.2, 133.8, 144.9, 196.3. **MS-EI** (m/z): 400(M^+).

Elemental analysis: Anal. Calcd for $C_{20}H_{32}O_4S_2$: C, 59.90, H, 8.05, S, 16.0; Found: C, 60.23, H, 8.25, S, 15.74.

Synthesis of **20 :** 1,6-Bis(toluene-4-sulfonyloxy)hexane (10 g, 24 mmol), 3,5-di-*tert*-butylphenol (4.4 g, 24 mmol) and K_2CO_3 (3.2 g, 24 mmol) in CH_3CN (200 ml) were heated and stirred at reflux overnight. The solvent was completely evaporated under vacuum, the solid residue was taken up with CH_2Cl_2 and H_2O. The separated organic layer was then washed with H_2O, dried over Na_2SO_4, and evaporated to dryness. The pure product was obtained by chromatography column (silica gel, hexane 70%-ethyl acetate 30%) as a white solid (yield 85%). **^{1}H NMR** ($CDCl_3$, 300 MHz,

ppm): δ 1.30(18H, s), 1.41(4H, m), 1.70(4H, m), 3.92(2H, J=6.4 Hz, t), 4.04(2H, J=6.4 Hz, t), 6.73(2H, J=1.5 Hz, d), 7.01(1H, J=1.5 Hz, t), 7.33(2H, J=8.3 Hz, d), 7.79(2H, J=8.3 Hz, d). **^{13}C NMR** ($CDCl_3$, 75 MHz, ppm): δ 25.1, 25.5, 28.7, 29.2, 31.4, 34.9, 67.3, 70.5, 108.7, 114.8, 127.8, 129.7, 152.1. **EI-MS** (m/z): 460(M^+). m.p.: 79-80 °C.

Elemental analysis: Anal. Calcd for $C_{27}H_{40}O_4S$: C, 70.39, H, 8.75, S, 6.96; Found: C, 70.77, H, 8.42, S, 7.22.

Synthesis of **21 :** Compound **20** (5.5 g, 12.5 mmol) and 4,4'-bipyridile (2 g, 12.5 mmol) were dissolved in CH_3CN (300 ml) and the resulting mixture was refluxed with stirring overnight. After cooling to room temperature, the solvent was completely evaporated under vacuum. The solid residue was then purified by recrystallization from acetone/ethyl acetate mixture as a white sticky solid. Yield 65%. **^{1}H NMR** ($CDCl_3$, 300 MHz, ppm): δ 1.28(20H, s), 1.41(2H, m), 1.67(2H, m), 1.94(2H, m), 2.25(3H, s), 3.87(2H, J=6 Hz, t), 4.75(2H, J=6 Hz, t), 6.70(2H, J=1.5 Hz, d), 6.99(1H, J=1.5 Hz, t), 7.08(2H, J=8 Hz, d), 7.55(2H, J=8 Hz, d), 7.73(2H, J=8 Hz, d), 8.18(2H, J=6.5 Hz, d), 8.73(2H, J=5.4 Hz), 9.21(2H, J=6.5 Hz, d). **^{13}C NMR** ($CDCl_3$, 75 MHz, ppm): δ 21.2, 25.4, 25.6, 29.5, 31.1, 31.4, 34.9, 61.5, 67.0, 108.6, 114.8, 121.4, 125.6, 125.8, 128.7, 139.4, 140.9, 143.5, 145.7, 150.6, 151.2, 152.1, 153.1, 158.4. **EI-MS** (m/z): 445(M^+). m.p.: 59-60 °C.

Elemental analysis: Anal. Calcd for $C_{37}H_{48}N_2O_4S$: C, 72.04, H, 8.11, N, 4.24, S, 4.89; Found: C, 71.84, H, 7.84, N, 4.54, S, 5.20.

Synthesis of **22** : **21** (2 g, 3.3 mmol) and **19** (1.4 g, 3.3 mmol) were dissolved in CH_3CN (70 ml). The mixture was heated and stirred at reflux for 5 days. The solvent was completely eliminated under vacuum and the white pure solid was obtained by precipitation in CH_3CN/ethyl acetate. Yield 50%. **^{1}H NMR** (CD_3OD, 300 MHz, ppm): δ 1.31-1.70(38H, m), 1.83(2H, m), 2.11(4H, m), 2.31(3H, s), 2.38(6H, s),2.86(2H, J=7 Hz, t), 3.99(2H, J=6 Hz, t), 4.75(4H, J=7 Hz, q), 6.70(2H, J=1.5 Hz, d), 7.03(1H, J=1.5 Hz, t), 7.23(4H, J=8 Hz, d), 7.70(4H, J=8 Hz, d), 8.66(4H, J=6.6 Hz, d), 9.27(4H, J_1=2 Hz J_2=4.8 Hz, dd). **^{13}C NMR** ($CDCl_3$, 75 MHz, ppm): δ 21.2, 25.5, 25.9, 26.0, 28.7, 28.9, 29.0, 29.2, 29.3, 29.4, 30.6, 31.4, 34.9, 61.9, 67.2, 108.6, 114.8, 125.7, 127.3, 128.8, 139.6, 143.3, 146.1, 148.7, 152.0, 158.5. **EI-MS** (m/z): 674(M^+), 337(M^+/2). m.p.: 160-162 °C.

Elemental analysis: Anal. Calcd for $C_{57}H_{80}N_2O_8S_3$: C, 67.23, H, 8.65, N, 2.75, S, 9.45; Found: C, 67.55, H, 8.53, N, 2.99, S, 9.10.

Synthesis of **23 :** Compound **22** (2 g, 2 mmol) was dissolved in CH_3OH (50 ml) then a solution of toluene-4-sulfonycacid (0.5 g, 2.5 mmol) in CH_3OH was added and the resulting mixture was heated and stirred overnight. The solvent was evaporated under vacuum and the pure white product was obtained by crystallization in CH_3CN. Yield 70%. **^{1}H NMR** ($CDCl_3$, 300 MHz, ppm): δ 1.00-1.50(36H, m), 1.60(4H, m), 1.80(4H, m), 2.26(6H, s), 2.49(2H, J=7 Hz, q), 3.85(2H, J=6 Hz, t), 4.61(4H, J=7 Hz, q), 6.71(2H, J=1.5 Hz, d), 6.99(1H, J=1.5 Hz, t), 7.10(4H, J=8 Hz, d), 7.70(4H, J=8 Hz, d), 8.79(4H, J=6.6 Hz, d), 9.21(4H, J=4.8 Hz, dd). **^{13}C NMR** ($CDCl_3$, 75 MHz, ppm): δ 21.2, 25.5, 25.7, 25.9, 26.0, 28.7,

28.9, 29.0, 29.1, , 29.4, 29.6, 34.9, 61.9, 67.2, 108.7, 114.8, 125.7, 127.3, 128.9, 139.6, 143.3, 145.8, 148.7, 152.1, 158.5. **EI-MS** (m/z): 632(M^+). m.p.: 189-191 ℃.

Elemental analysis: Anal. Calcd for $C_{55}H_{78}N_2O_7S_3$: C, 67.72, H, 8.06, N, 2.90, S, 9.86; Found: C, 67.91, H, 7.85, N, 3.18, S, 10.13.

Acknowledgment

In primis vorrei ringraziare coloro i quali hanno permesso la realizzazione di questa tesi e che mi hanno dovuto sopportare in questi 4 anni di lavoro al laboratorio 49. Grazie al **Dr. Andrea Secchi**, al **Prof. Andrea Pochini** ed al **Prof. Arturo Arduini**. Grazie per avermi insegnato la "vera" chimica e per aver sempre cercato il meglio in ogni cosa fatta, questa lunga esperienza è stata importante anche grazie a voi.

Non posso certo non salutare e ringraziare tutti coloro che mi hanno fatto compagnia in laboratorio: **Giovanni** (il Chiarissimo, grazie per la tua amicizia e per le grandi partite di calcetto), **Fabio** (il pettegolo(vabbè potrei metterne altri ma è meglio tralasciare)), **Luca** (sgaggioman… letteralmente un mito), **Rocco**, **Nutella** (Marcello), **Gloria**, **Alessandro** e **Cristina**. Grazie per le belle cene passate insieme e per avermi fatto sempre sentire in una grande famiglia!

A special thanks goes obviously to **Dr. Anton Plech, Dr. Vassilios Kotaidis** and **Andreas Sims** of the Univeristy of Konstanz. Thank you very much for the great experience I made and for trying(not always successfully) to make me understand Physics. Vielen Dank auch für den leckeren Grill.

Un grande abbraccio va ai miei compagni di avventure in questi anni univeristari parmensi: **Nas** (Lorenzo??) (sei un'uomo buono lo sai vero??), **Marcello** (sei e rimarrai sempre un'indegno… fatti un

Montenegro alla mia salute vah), **Marco**(il mio coinquilino preferito… senza di te questi ultimi anni non sarebbero stati gli stessi), **Monica** (una persona davvero speciale e che è riuscita a sopportare un gruppo di dementi come noi), **Lucia** (Puccia colei che deve sopportare Birimbardi e che non contenta c'è pure andata a convivere… ti ammiro), **Luca** (l'uomo serio che cmq ha sempre tirato fuori un soriso nei momenti importanti, verrò ad una fiera dei fumetti prima o poi), **Giovanni** (il cazzeggiatore per eccellenza), **Roger** (grazie per le serate all'etere a casa) e **Paolo** (mr.tecnologia…ma che ha un pc che non legge i file video!!).
Un grande grazie è anche per i miei amici di ormai lunga data di Bolzano : in particolare **Miki**, **Robi**, **Paolo** e **Astrid**. Grazie delle belle serate insieme e per essere sempre allegri e felici.

Un grazie enorme va di sicuro ai miei genitori **Lucia** (Mà) e **Bruno** (Pà). Grazie per essermi sempre stato accanto in ogni passo della mia vita e per avermi aiutato in tutto. Grazie per avermi appoggiato in ogni cosa che ho fatto e per avermi sempre consigliato al meglio. Vi voglio bene!!

Ed infine vorrei ringraziare la mia "FIDANZATA" **Michela** : questi anni senza di te non sarebbero stati possibili! Mi sei stata sempre vicina e mi hai aiutato in qualsiasi cosa che ho fatto. Hai sopportato con me la lunga distanza e mi hai regalato sempre un grande sorriso nei momenti difficili. Grazie per tutte le cose che hai detto e fatto per rendermi una persona migliore e per aver, in fin dei conti, sempre creduto in me. Grazie insomma per essermi accanto e per tutto quello che verrà in futuro! Sei fantastica!!